

Charm mixing from BABAR^{*}

N. Neri¹⁾ (for the BABAR Collaboration)

(BABAR Collaboration, Università di Pisa and INFN, L. Bruno Pontecorvo 3, 56127 Pisa, Italy)

Abstract We present recent results from BABAR experiment for D^0 - \bar{D}^0 mixing measurements. Mixing parameters can be measured in different ways using different D^0 decay modes, here we discuss the most sensitive analyses such as $D^0 \rightarrow K^+\pi^-$ where we had the first evidence of charm mixing, the measurement of the ratio of lifetimes of the decays $D^0 \rightarrow K^+K^-$ and $D^0 \rightarrow \pi^+\pi^-$ relative to $D^0 \rightarrow K^-\pi^+$, the time dependent Dalitz plot analysis of $D^0 \rightarrow K^+\pi^-\pi^0$. New limits on CP -violating time-integrated asymmetries in $D^0 \rightarrow K^+K^-$ and $D^0 \rightarrow \pi^+\pi^-$ are also discussed. The analyses presented are based on 384 fb^{-1} data collected with the BABAR detector at the PEP-II asymmetric B Factory.

Key words charm mixing, flavor oscillations, D^0 mesons, BABAR

PACS 12.15.Ff, 13.25.Ft, 11.30.Er

1 Introduction

D^0 - \bar{D}^0 oscillations can be explained by the fact that the Hamiltonian which determines the time-evolution of the neutral D meson system is not diagonal in the flavor defined base. The simplified time evolution is determined by a 2×2 effective hamiltonian matrix $\mathcal{H} = \mathbf{M} - \frac{i}{2}\mathbf{\Gamma}$ by solving the the Schrödinger equation:

$$i\frac{\partial}{\partial t} \begin{pmatrix} D^0(t) \\ \bar{D}^0(t) \end{pmatrix} = \left(\mathbf{M} - \frac{i}{2}\mathbf{\Gamma} \right) \begin{pmatrix} D^0(t) \\ \bar{D}^0(t) \end{pmatrix}, \quad (1)$$

where D^0 and \bar{D}^0 are the neutral D mesons of opposite flavor content and \mathbf{M} and $\mathbf{\Gamma}$ are the Hermetian matrices which represent the dispersive (mass) and absorbitive (widths) parts of the contribution to the flavor mixing. The eigenstates of the effective Hamiltonian, $|D_{1,2}\rangle$, are therefore a linear combination of $|D^0\rangle$ and $|\bar{D}^0\rangle$:

$$|D_{1,2}\rangle = p|D^0\rangle \pm q|\bar{D}^0\rangle, \quad \text{with } |p|^2 + |q|^2 = 1. \quad (2)$$

p , q are related to the eigenvalues of the effective hamiltonian. The time evolution is well defined:

$$|D_{1,2}(t)\rangle = e_{1,2}(t)|D_{1,2}\rangle, \quad (3)$$

$$e_{1,2}(t) = \exp \left[-i(m_{1,2} - \frac{i\Gamma_{1,2}}{2})t \right], \quad (4)$$

where $m_{1,2}$ and $\Gamma_{1,2}$ are the masses and the widths of the hamiltonian eigenstates. If CP is conserved, then $p = q = 1$ and the physical states are CP eigenstates.

The state $|D^0\rangle$ evolves in time as

$$|D^0(t)\rangle = e^{-(\bar{\Gamma}/2 + i\bar{m})t} \left[\cosh[(y + ix)\bar{\Gamma}t/2]|D^0\rangle - \frac{q}{p} \sinh[(y + ix)\bar{\Gamma}t/2]|\bar{D}^0\rangle \right], \quad (5)$$

where $\bar{m} = (m_1 + m_2)/2$ and $\bar{\Gamma} = (\Gamma_1 + \Gamma_2)/2$. The mixing parameters x and y are defined as

$$x \equiv \frac{m_1 - m_2}{\bar{\Gamma}}, \quad y \equiv \frac{\Gamma_1 - \Gamma_2}{2\bar{\Gamma}}. \quad (6)$$

As can be seen from Eq. (5), an opposite flavor component appears after some time t if either x or y is non-zero.

The effects of CP violation (CPV) in D^0 - \bar{D}^0 mixing can be parameterized in terms of the quantities

$$r_m \equiv \left| \frac{q}{p} \right| \quad \text{and} \quad \varphi_f \equiv \arg \left(\frac{q \bar{A}_f}{p A_f} \right), \quad (7)$$

where $A_f \equiv \langle f | \mathcal{H}_D | D^0 \rangle$ ($\bar{A}_f \equiv \langle f | \mathcal{H}_D | \bar{D}^0 \rangle$) is the amplitude for D^0 (\bar{D}^0) to decay into a final state f , and \mathcal{H}_D is the Hamiltonian for the decay. A value of $r_m \neq 1$ would indicate CP violation in mixing. A non-zero value of φ_f would indicate CPV in the interference of mixing and decay.

Received 5 February 2008

^{*} Supported by Università di Pisa and INFN. Also Supported by U.S. Department of Energy and SLAC, Stanford University

1) E-mail: nicola.neri@pi.infn.it

In the Standard Model (SM) D^0 - \bar{D}^0 oscillations are predicted to proceed quite slowly. The short distance contributions to D^0 - \bar{D}^0 mixing from the SM box diagrams are expected to be very small^[1, 2]. Long-distance effects from intermediate states coupling to both D^0 and \bar{D}^0 are expected to contribute, but are difficult to estimate precisely^[3].

Within the SM, CP violation is also expected to be small in the D^0 - \bar{D}^0 system. An observation of CPV in D^0 - \bar{D}^0 mixing with the present experimental sensitivity would be evidence for physics beyond the SM^[4].

Recent results from BABAR^[5] and BELLE^[6] show an evidence of D^0 - \bar{D}^0 oscillation at 3.9σ and 3.2σ level respectively. At this level of precision the measurements are compatible with the predicted values from SM and put significant constraints on new physics models^[2, 7].

2 Selection of D^0 signal events

Signal events are selected via the cascade decay $D^{*+} \rightarrow D^0\pi_s^{+1}$, in this way the flavor of the D meson, at $t = 0$, is identified by the charge of the soft pion (π_s). The difference of the reconstructed D^{*+} and D^0 masses (Δm), which has an experimental resolution at the level of ≈ 350 keV/ c^2 , is used to remove background events by requiring to be less than 1 MeV/ c^2 from the expected value, 145.5 MeV/ c^2 ^[8]. In order to reject background events with D^0 candidates from B meson decays, we require the momentum of the D^0 , evaluated in the center-of-mass (CM) of the e^+e^- system, to be greater than 2.4 GeV/ c . Reconstructed D^0 events are therefore produced in the process $e^+e^- \rightarrow c\bar{c}$ which has a cross section of 1.3 nb at a CM energy close to 10.6 GeV. The D^0 proper-time, t , is determined in a vertex constrained combined fit to the D^0 production and decay vertices. In this fit the D^0 and the π_s tracks are imposed to originate from the e^+e^- luminous region. The average error on the proper time, $\sigma_t \sim 0.2$ ps, is comparable with half of the D^0 lifetime^[8]. Particle identification algorithms are used to identify the charged tracks from D^0 decays.

3 Evidence for D^0 - \bar{D}^0 mixing in wrong-sign decays $D^0 \rightarrow K^+\pi^-$

We present the measurement of the D^0 - \bar{D}^0 mixing with a time-dependent analysis of the wrong-sign (WS) decays $D^0 \rightarrow K^+\pi^-$ ^[5]. The final WS state can be produced via the doubly Cabibbo-suppressed (DCS)

decay or via mixing followed by the Cabibbo-favored (CF) decay $D^0 \rightarrow \bar{D}^0 \rightarrow K^+\pi^-$. The time dependence of the WS decay of a meson produced as a D^0 at time $t = 0$ in the limit of small mixing ($|x|, |y| \ll 1$) and CP conservation can be approximated as

$$\frac{T_{\text{WS}}(t)}{e^{-\Gamma t}} \propto R_D + \sqrt{R_D} y' \bar{\Gamma} t + \frac{x'^2 + y'^2}{4} (\bar{\Gamma} t)^2, \quad (8)$$

where R_D is the ratio of doubly Cabibbo-suppressed to Cabibbo-favored (CF) decay rates, $x' = x \cos \delta_{K\pi} + y \sin \delta_{K\pi}$, $y' = -x \sin \delta_{K\pi} + y \cos \delta_{K\pi}$, and $\delta_{K\pi}$ is the strong phase between the DCS and CF amplitudes.

The time dependence of the WS decays is used to separate the contribution of DCS decays from that of D^0 - \bar{D}^0 mixing. The mixing parameters are determined by an unbinned extended maximum-likelihood fit to the reconstructed D^0 invariant mass m_{D^0} , Δm , t , σ_t variables for WS decays. After applying the selection criteria we retain approximately 1 229 000 RS and 6400 WS D^0 and \bar{D}^0 candidates. The CF or right sign (RS) decays are used to extract the shapes of signal and background events together with the lifetime and proper time resolution function. In Fig. 1 is reported the proper time distribution for WS events, background components are shown as shaded regions. The fit results with and without mixing are shown as the overlaid curves.

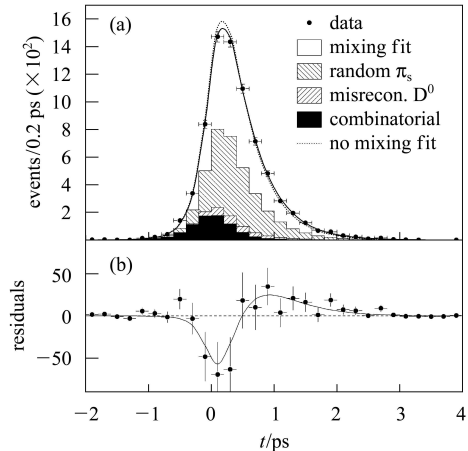


Fig. 1. (a) The proper-time distribution of combined D^0 and \bar{D}^0 WS candidates in the signal region $1.843 < m_{K\pi} < 1.883$ GeV/ c^2 and $0.1445 < \Delta m < 0.1465$ GeV/ c^2 . The result of the fit allowing (not allowing) mixing but not CP violation is overlaid as a solid (dashed) curve. Background components are shown as shaded regions. (b) The points represent the difference between the data and the no-mixing fit. The solid curve shows the difference between fits with and without mixing.

The fit which allows for mixing is substantially giving a better description of the data. The significance of the mixing is evaluated based on the change

1) Consideration of charge conjugation is implied throughout this paper, unless otherwise stated.

in the negative log likelihood with respect to the minimum and the confidence level countours including systematic errors are shown in Fig. 2, where the no-mixing point (x'^2, y') \equiv (0,0) is shown as a plus sign (+).

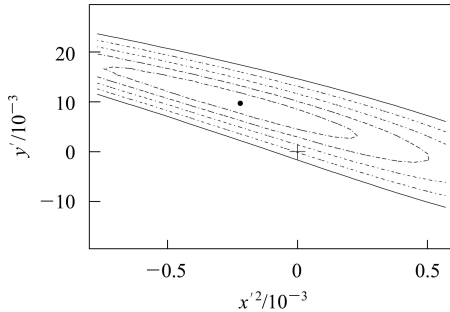


Fig. 2. The central value (point) and confidence-level (CL) contours for $1 - \text{CL} = 0.317$ (1σ), 4.55×10^{-2} (2σ), 2.70×10^{-3} (3σ), 6.33×10^{-5} (4σ) and 5.73×10^{-7} (5σ), calculated from the change in the value of $-2\ln\mathcal{L}$ compared with its value at the minimum. Systematic uncertainties are included. The no-mixing point is shown as a plus sign (+).

We have performed fits to the WS proper time distribution using three different models. The first model doesn't allow for mixing or CPV and fit for the parameter R_D , the second model allows for mixing assuming CP is conserved and measures R_D , x'^2 and y' while the third model allows for mixing and CPV . To search for CP violation, we apply Eq. (8) to D^0 and \bar{D}^0 samples separately, fitting for the parameters $\{R_D^\pm, x'^{2\pm}, y'^{\pm}\}$ for D^0 (+) decays and \bar{D}^0 (-) decays, and we introduce the parameters $R_D = \sqrt{R_D^+ R_D^-}$ and $A_D = (R_D^+ - R_D^-)/(R_D^+ + R_D^-)$.

Table 1. Results from the different fits. The first uncertainty listed is statistical and the second systematic.

fit type	parameter	fit results ($/10^{-3}$)
no CPV or mixing	R_D	$3.53 \pm 0.08 \pm 0.04$
no CPV	R_D	$3.03 \pm 0.16 \pm 0.10$
	x'^2	$-0.22 \pm 0.30 \pm 0.21$
	y'	$9.7 \pm 4.4 \pm 3.1$
CPV allowed	R_D	$3.03 \pm 0.16 \pm 0.10$
	A_D	$-21 \pm 52 \pm 15$
	x'^{2+}	$-0.24 \pm 0.43 \pm 0.30$
	y'^+	$9.8 \pm 6.4 \pm 4.5$
	x'^{2-}	$-0.20 \pm 0.41 \pm 0.29$
	y'^-	$9.6 \pm 6.1 \pm 4.3$

The largest contribution to systematic error is due to uncertainty in modeling the long decay time component from other D decays in the signal region. The second largest component, is due to the presence of a non-zero mean in the proper time signal resolution.

The systematic error on A_D is primarily due to uncertainties in modeling the differences between K^+ and K^- absorption in the detector.

The results of the three different fits including statistical and systematic errors are reported in Table 1.

4 Lifetime ratio analysis

One consequence of D^0 - \bar{D}^0 mixing is that D^0 decay time distribution can be different for decays to different CP eigenstates. D^0 - \bar{D}^0 mixing will alter the decay time distribution of D^0 and \bar{D}^0 mesons that decay into final states of specific CP [9]. To a good approximation, these decay time distributions can be treated as exponential with effective lifetimes τ_{hh}^+ and τ_{hh}^- , given by^[10]

$$\tau_{hh}^+ = \tau_{K\pi} / [1 + r_m (y \cos \varphi_f - x \sin \varphi_f)], \quad (9)$$

$$\tau_{hh}^- = \tau_{K\pi} / [1 + r_m^{-1} (y \cos \varphi_f + x \sin \varphi_f)],$$

where $\tau_{K\pi}$ is the lifetime for the Cabibbo-favored decays $D^0 \rightarrow K^- \pi^+$ and $\bar{D}^0 \rightarrow K^+ \pi^-$, and τ_{hh}^+ (τ_{hh}^-) is the lifetime for the Cabibbo-suppressed decays of the D^0 (\bar{D}^0) into CP -even final states (such as $K^- K^+$ and $\pi^- \pi^+$). These effective lifetimes can be combined into the quantities y_{CP} and ΔY :

$$y_{CP} = \frac{\tau_{K\pi}}{\langle \tau_{hh} \rangle} - 1, \quad (10)$$

$$\Delta Y = \frac{\tau_{K\pi}}{\langle \tau_{hh} \rangle} A_\tau,$$

where $\langle \tau_{hh} \rangle = (\tau_{hh}^+ + \tau_{hh}^-)/2$ and $A_\tau = (\tau_{hh}^+ - \tau_{hh}^-)/(\tau_{hh}^+ + \tau_{hh}^-)$. Both y_{CP} and ΔY are zero if there is no D^0 - \bar{D}^0 mixing. In the limit where CP is conserved in mixing and decay, but violated in the interference between them, these quantities are related to the mixing parameters $y_{CP} = y \cos \varphi_f$ and $\Delta Y = x \sin \varphi_f$, with the convention that $\cos \varphi_f > 0$.

We measure the D^0 lifetime in the three different D^0 decay modes, $K^- \pi^+$, $K^- K^+$ and $\pi^+ \pi^-$, and use the charge of the parent $D^{*\pm}$ to split the $K^- K^+$ and $\pi^+ \pi^-$ samples into those originating from D^0 and from \bar{D}^0 mesons for measuring the CP -violating parameters^[11]. In order to reduce systematic errors to the minimum, the event selection was chosen to produce very pure signal samples. The event yields and purities of the signal candidate samples (those with invariant masses satisfying $1.8495 < m_{D^0} < 1.8795$ GeV/ c^2) are listed in Table 2.

Table 2. Event yields and purities of the tagged D^0 samples calculated inside the signal region.

sample	size	purity
$K^- \pi^+$	730 880	99.9%
$K^- K^+$	69 696	99.6%
$\pi^- \pi^+$	30 679	98.0%

The proper time distribution is fit to an exponential convolved with the detector resolution function.

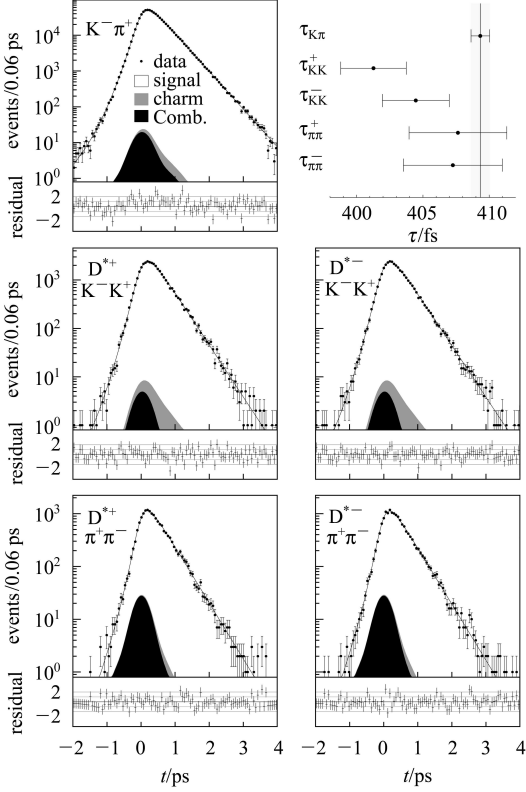


Fig. 3. Decay time distribution in the data samples with the combined fit overlaid. The top left plot is the tagged $K^-\pi^+$ sample, the middle plots are the D^{*+} (left) and D^{*-} (right) tagged K^-K^+ samples, and the bottom plots are the tagged $\pi^+\pi^-$ samples. The shaded and black distributions represent the background expected in the fit. The normalized residuals for each fit are shown as a separate histogram for each sample. The top right plot shows a summary of the measured lifetimes.

Table 3. The mixing parameters extracted from the fit to data. The first error is statistical and the second systematic.

sample	y_{CP}	ΔY
K^-K^+	$(1.60 \pm 0.46 \pm 0.17)\%$	$(-0.40 \pm 0.44 \pm 0.12)\%$
$\pi^+\pi^-$	$(0.46 \pm 0.65 \pm 0.25)\%$	$(0.05 \pm 0.64 \pm 0.32)\%$
combined	$(1.24 \pm 0.39 \pm 0.13)\%$	$(-0.26 \pm 0.36 \pm 0.08)\%$

The results of the lifetime fits are shown in Fig. 3. The fitted D^0 lifetime $\tau_{K\pi}$ is found to be 409.33 ± 0.70 (stat) fs, consistent with the world-average lifetime^[8]. From the fit results we calculate y_{CP} and ΔY for the K^-K^+ mode, the $\pi^+\pi^-$ mode, and the two modes combined, where the combined result is obtained assuming $\tau_{K^+K^-}^+ = \tau_{\pi^+\pi^-}^+$ and $\tau_{K^+K^-}^- = \tau_{\pi^+\pi^-}^-$. The y_{CP} and ΔY

results are listed in Table 3. In particular the measurement of $y_{CP} = (1.24 \pm 0.39 \pm 0.13)\%$ is evidence of $D^0-\bar{D}^0$ mixing at 3σ level.

The systematic uncertainties on the mixing parameters are small, since most uncertainties in the lifetimes cancel in the ratios. We have considered variations in the signal and background fit models, changes to the event selection and detector effects that could introduce biases in the lifetime. Table 4 summarizes the various systematic uncertainties.

Table 4. Summary of systematic uncertainties on y_{CP} and ΔY , separately for K^-K^+ and $\pi^+\pi^-$ and averaged over the two CP modes, in percent.

systematic	$\sigma_{y_{CP}} (\%)$		
	K^-K^+	$\pi^+\pi^-$	Av.
signal model	0.130	0.059	0.085
charm bkg.	0.062	0.037	0.043
combinatoric bkg.	0.019	0.142	0.045
selection criteria	0.068	0.178	0.046
detector model	0.064	0.080	0.064
quadrature sum	0.172	0.251	0.132

systematic	$\sigma_{\Delta Y} (\%)$		
	K^-K^+	$\pi^+\pi^-$	Av.
signal model	0.072	0.265	0.062
charm bkg.	0.001	0.002	0.001
combinatoric bkg.	0.001	0.005	0.002
selection criteria	0.083	0.172	0.011
detector model	0.054	0.040	0.054
quadrature sum	0.122	0.318	0.083

The results shown in Table 3 have been combined with a previous BABAR study^[12] based on 91 fb^{-1} of data. That analysis does not require a D^* to identify the D^0 decay as the analysis presented here, the two event samples are essentially disjoint and can be considered statistically independent. The combined result is $y_{CP} = [1.03 \pm 0.33(\text{stat}) \pm 0.19(\text{syst})]\%$.

5 Measurement of $D^0-\bar{D}^0$ mixing in the decay $D^0 \rightarrow K^+ \pi^- \pi^0$

In this section, we present a study of the WS decays $D^0 \rightarrow K^+ \pi^- \pi^0$ in which the flavor of the D^0 meson is known at its production time. The WS decays are analyzed with a time-dependent Dalitz plot technique to distinguish the DCS contribution from the CF contribution originating from mixing. Assuming CP conservation and for small values of x and y , the time-dependent WS decay rate as a function of the Dalitz variables $s_{12} = m_{K^+\pi^-}^2$ and $s_{13} = m_{K^+\pi^0}^2$ and decay time t is given by:

$$\Gamma_{\bar{f}}(s_{12}, s_{13}, t) = e^{-\Gamma t} \{ |A_{\bar{f}}(s_{12}, s_{13})|^2 + |A_{\bar{f}}(s_{12}, s_{13})| |\bar{A}_{\bar{f}}(s_{12}, s_{13})| [y'' \cos \delta_{\bar{f}}(s_{12}, s_{13}) - x'' \sin \delta_{\bar{f}}(s_{12}, s_{13})] (\Gamma t) + \frac{x''^2 + y''^2}{4} |\bar{A}_{\bar{f}}(s_{12}, s_{13})|^2 (\Gamma t)^2 \}, \quad (11)$$

where $\bar{f} = K^+\pi^-\pi^0$, $A_{\bar{f}} = \langle \bar{f} | \mathcal{H} | D^0 \rangle$ and $\bar{A}_{\bar{f}} = \langle \bar{f} | \mathcal{H} | \bar{D}^0 \rangle$ are the decay amplitudes for the DCS and CF transitions, respectively, and $\delta_{\bar{f}}(s_{12}, s_{13}) = \arg[A_{\bar{f}}^*(s_{12}, s_{13}) \bar{A}_{\bar{f}}(s_{12}, s_{13})]$. The decay distribution is sensitive to $y'' = y \cos \delta_{K\pi\pi^0} - x \sin \delta_{K\pi\pi^0}$ and $x'' = x \cos \delta_{K\pi\pi^0} + y \sin \delta_{K\pi\pi^0}$ where $\delta_{K\pi\pi^0}$ is the strong-phase difference between the CF and the DCS decay amplitudes and cannot be determined in the analysis of these decays alone.

The CF amplitude $\bar{A}_{\bar{f}}$ is determined up to an overall phase and arbitrary amplitude in a time-independent Dalitz plot analysis of RS decays. The DCS amplitude $A_{\bar{f}}$ together with the parameters x'' and y'' are determined in a time-dependent Dalitz plot analysis of WS decays. In the Dalitz analysis, the CF and DCS amplitudes are parameterized using an isobar model^[13].

Signal and backgrounds are distinguished by their differing shapes in Δm and $m_{K\pi\pi^0}$. The backgrounds considered are (1) correctly reconstructed D^0 candidates paired with a random π_s (“mistag” events); (2) D^{*+} decays with a correct π_s^+ and a misreconstructed D^0 (“bad- D^0 ”); and (3) combinatorial background. The signal and background yields in the Dalitz analysis signal region $1.85 < m_{K\pi\pi^0} < 1.88 \text{ GeV}/c^2$ and $0.145 < \Delta m < 0.146 \text{ GeV}/c^2$ are shown in Table 5. The purity of the RS sample in this region is approximately 99%.

Table 5. Number of RS and WS signal and background events in the $m_{K\pi\pi^0}$ and Δm signal region defined by $0.145 < \Delta m < 0.146 \text{ GeV}/c^2$ and $1.85 < m_{K\pi\pi^0} < 1.88 \text{ GeV}/c^2$.

category	RS events	WS events
signal	639802 ± 1538	1483 ± 56
combinatoric	1537 ± 57	499 ± 57
mistag	2384 ± 57	765 ± 29
bad- D^0	3117 ± 93	227 ± 75

The total PDF for the WS Dalitz fit is given by

$$P(t, m_{K^+\pi^-}, m_{K^+\pi^0}) = N_{\text{sig}} P_{\text{sig}} + N_{\text{mistag}} P_{\text{mistag}} + N_{\text{bad-}D^0+\text{comb}} P_{\text{bad-}D^0+\text{comb}}, \quad (12)$$

where the yields for signal, N_{sig} , mistag background, N_{mistag} and sum of mis-reconstructed D^0 and combinatoric backgrounds, $N_{\text{bad-}D^0+\text{comb}}$, are taken from Table 5. The signal PDF, P_{sig} , given by Eq. (11)

is convolved with a decay time resolution function determined from fitting the RS data. The CF amplitudes and phases are fixed from the RS fit. The PDF P_{mistag} for mistag events consists of the RS Dalitz model times an exponential convolved with the RS decay time resolution. The results of the time-dependent Dalitz fit to the WS data sample are listed in Table 6. The WS decay proceeds primarily through $D^0 \rightarrow K^+\rho(770)^-$ and $D^0 \rightarrow K^*(892)^+\pi^-$. In Fig. 4(a) is shown the proper time distribution for the WS sample. The Dalitz plot projections of the WS data with the fit results overlaid are shown in Fig. 4(b), (c).

Table 6. Dalitz fit results for the WS D^0 data sample. The total fit fraction is 102 % and $\chi^2/\text{ndof} = 188/215 = 0.876$. With a_i we indicate the amplitude, with δ_i the phase and with f_i the fit fraction of the resonance i of the isobar model for the DCS decay.

resonance	a_i	$\delta_i/\text{degrees}$	f_i (%)
$\rho(770)$	1 (fixed)	0 (fixed)	39.8 ± 6.5
$K_2^{*0}(1430)$	0.088 ± 0.017	-17.2 ± 12.9	2.0 ± 0.7
$K_0^{*+}(1430)$	6.78 ± 1.00	69.1 ± 10.9	13.1 ± 3.3
$K^{*+}(892)$	0.899 ± 0.005	-171.0 ± 5.9	35.6 ± 5.5
$K_0^{*0}(1430)$	1.65 ± 0.59	-44.4 ± 18.5	2.8 ± 1.5
$K^{*0}(892)$	0.398 ± 0.038	24.1 ± 9.8	6.5 ± 1.4
$\rho(1700)$	5.4 ± 1.6	157.4 ± 20.3	2.0 ± 1.1

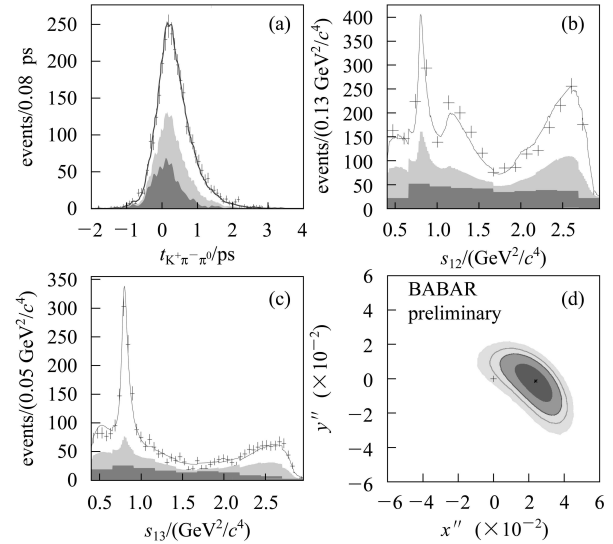


Fig. 4. Fit projections for the WS sample. The light histogram represents the mistag background, the dark histogram the combinatoric background while the line represents the fit results to the data (points with error bars). In (a) is shown the D^0 proper time distribution. The Dalitz projections for s_{12} and s_{13} are shown in (b) and (c) respectively. In (d) is shown the probability contour for x'' and y'' in the case of CP conservation. The contours refer to 68.3%, 95.0%, 99.0%, 99.9% probability respectively.

The mixing parameters determined from the WS fit are shown in Table 7. No evidence of CPV was found when fitting separately for D^0 and \bar{D}^0 events to search for CP violation effects in mixing. From these values, we determine the time-integrated mixing rate to be:

$$R_{\text{mix}} = (x''^2 + y''^2)/2 = (x^2 + y^2)/2 = (2.9 \pm 1.6) \times 10^{-4},$$

where the error includes both statistical and systematic uncertainties. The major sources of systematic error on the mixing parameters include uncertainties in modeling the background decay time distribution in the signal region, uncertainties in the mass and width of each resonance in the Dalitz model, the values chosen for the decay time and decay time error selection criteria, uncertainties in modeling the decay time signal resolution function and uncertainties in determining $N_{\text{bad}-D^0+\text{comb}}$.

Table 7. Mixing parameters from time-dependent WS Dalitz analysis. The first error is statistical, the second systematic. The linear correlation between them is -0.34 .

quantity	value
x''	$(-2.39 \pm 0.61(\text{stat}) \pm 0.32(\text{syst}))\%$
y''	$(-0.14 \pm 0.60(\text{stat}) \pm 0.40(\text{syst}))\%$

The probability contour plots for x'' and y'' are shown in Fig. 4(d). From the change in log-likelihood between the best fit value and the no-mix (x'', y'') = (0,0) point, the data are consistent with the no-mixing hypothesis at the 0.1% level, including systematic uncertainties.

6 Search for CPV in the decays $D^0 \rightarrow K^-K^+$ and $D^0 \rightarrow \pi^-\pi^+$

Within the SM, CPV asymmetries in the decays $D^0 \rightarrow K^-K^+$ and $D^0 \rightarrow \pi^-\pi^+$ are predicted to be $\mathcal{O}(0.001\%-0.01\%)^{[1, 14]}$. The observation of CP asymmetries at the level of current experimental sensitivity^[15] would indicate a clear sign of physics beyond the SM^[2, 16]. We report on a search for CPV in neutral D mesons^[17], produced from the reaction $e^+e^- \rightarrow c\bar{c}$, by measuring the time-integrated asymmetries

$$a_{CP}^{\text{hh}} = \frac{\Gamma(D^0 \rightarrow h^+h^-) - \Gamma(\bar{D}^0 \rightarrow h^+h^-)}{\Gamma(D^0 \rightarrow h^+h^-) + \Gamma(\bar{D}^0 \rightarrow h^+h^-)}, \quad (13)$$

where $h = K$ or π .

In this construction, a_{CP}^{hh} , includes all CP violating contributions, direct and indirect^[16].

In order to measure the CP asymmetry, we have to account and correct for detector-related asymmetries. Besides the tagging asymmetry for D^0 and \bar{D}^0 via $D^{*\pm}$ decays, the forward backward (FB) asymmetry in $e^+e^- \rightarrow c\bar{c}$ production will create a difference

in the number of D^0 and \bar{D}^0 reconstructed due to the FB detection asymmetry due to the boost of the CM system relatively to the laboratory.

To correct for asymmetry in this flavor tag, we measure the relative efficiency for detecting soft pions in recorded data using both tagged and untagged $D^0 \rightarrow K^-\pi^+$ samples.

To separate CP asymmetry from FB asymmetry, we calculate yield asymmetries as a function of $\cos\theta \equiv \cos\theta_{D^0}^{\text{CMS}}$ and project out the even and odd parts. We define

$$a^\pm(\cos\theta) = \frac{n_{D^0}(\pm|\cos\theta|) - n_{\bar{D}^0}(\pm|\cos\theta|)}{n_{D^0}(\pm|\cos\theta|) + n_{\bar{D}^0}(\pm|\cos\theta|)}, \quad (14)$$

$$a_{CP}(\cos\theta) \approx (a^+(\cos\theta) + a^-(\cos\theta))/2, \quad (15)$$

$$a_{\text{FB}}(\cos\theta) \approx (a^+(\cos\theta) - a^-(\cos\theta))/2. \quad (16)$$

where n_{D^0} and $n_{\bar{D}^0}$ are the numbers of signal events for D^0 and \bar{D}^0 , a_{CP} the even component and $a_{\text{FB}}(\cos\theta)$ the odd component. The even part represents CP -violating effects, the odd part the production asymmetry, including higher-order QED contributions. The asymmetries $a_{CP}(\cos\theta)$ and a_{FB} are shown in Fig. 5. The measured asymmetries are listed in Table 8. The contributions to the systematic errors are listed in Table 9.

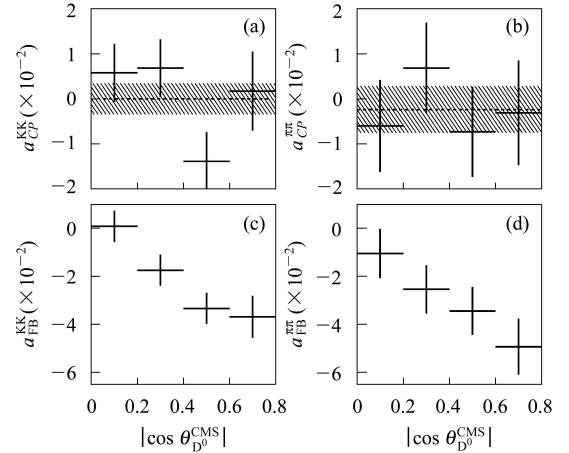


Fig. 5. CP -violating asymmetries in (a) KK and (b) $\pi\pi$, and forward-backward asymmetries in (c) KK and (d) $\pi\pi$. In (a) and (b), the dashed lines represent the central values and the hatched regions the 1σ intervals, obtained from χ^2 minimizations.

Table 8. CPV asymmetries. The first error is statistical, the second systematic.

quantity	value
a_{CP}^{KK}	$(0.00 \pm 0.34 \pm 0.13)\%$
$a_{CP}^{\text{pi pi}}$	$(-0.24 \pm 0.52 \pm 0.22)\%$

Table 9. Summary of systematic uncertainties on a_{CP}^{hh} .

category	Δa_{CP}^{KK}	$\Delta a_{CP}^{\pi\pi}$
2-Dim. PDF shapes	$\pm 0.04\%$	$\pm 0.05\%$
π_s correction	$\pm 0.08\%$	$\pm 0.08\%$
a_{CP} extraction	$\pm 0.09\%$	$\pm 0.20\%$
quadrature sum	$\pm 0.13\%$	$\pm 0.22\%$

7 Conclusions

We have presented recent results from BABAR experiment based on a data sample of 384 fb^{-1} for the measurements of D^0 - \bar{D}^0 mixing. We have found evidence of mixing in the time dependent analysis of the WS $D^0 \rightarrow K^+\pi^-$ decays, measuring $x'^2 = [-0.22 \pm 0.30(\text{stat}) \pm 0.21(\text{syst})]\%$ and $y' = [9.7 \pm 4.4(\text{stat}) \pm 3.1(\text{syst})]\%$ which represents evidence of mixing at 3.9σ level. No evidence for CPV was

found in this analysis. In an analysis measuring the lifetimes $\tau(D^0 \rightarrow K^-\pi^+)$, $\tau(D^0 \rightarrow K^+K^-)$ and $\tau(D^0 \rightarrow \pi^+\pi^-)$ we have obtained a value of $y_{CP} = [1.24 \pm 0.39(\text{stat}) \pm 0.13(\text{syst})]\%$ which is evidence of D^0 - \bar{D}^0 mixing at the 3σ level. We determine the CP violation parameter ΔY to be $[-0.26 \pm 0.36(\text{stat}) \pm 0.08(\text{syst})]\%$. In a time-dependent Dalitz analysis of WS decays $D^0 \rightarrow K^+\pi^-\pi^0$, we extract the parameters $x'' = [2.39 \pm 0.61(\text{stat}) \pm 0.32(\text{syst})]\%$ and $y'' = [-0.14 \pm 0.60(\text{stat}) \pm 0.40(\text{syst})]\%$. These values are consistent with no-mixing at a probability of 0.8%. We also measure the time-integrated CP asymmetries a_{CP}^{hh} , $h = K$ or π , and obtain $a_{CP}^{KK} = [0.0 \pm 0.34(\text{stat}) \pm 0.13(\text{syst})]\%$ and $a_{CP}^{\pi\pi} = [-0.24 \pm 0.52(\text{stat}) \pm 0.22(\text{syst})]\%$. At the precision of these measurements, there is no evidence of CPV in either of the CP -even D^0 decay modes investigated. The values of the CP asymmetries are consistent with SM expectations.

References

- 1 Bianco S et al. Riv. Nuovo Cim., 2003, **26N7**: 1. hep-ex/0309021
- 2 Burdman G, Shipsey I. Ann. Rev. Nucl. Part. Sci., 2003, **53**: 431
- 3 Wolfenstein L. Phys. Lett. B, 1985, **164**: 170; Donoghue J F et al. Phys. Rev. D, 1986, **33**: 179; Bigi I I Y, Uraltsev N G. Nucl. Phys. B, 2001, **592**: 92. hep-ph/0005089; Falk A F et al. Phys. Rev. D, 2002, **65**: 054034. hep-ph/0110317; Falk A F et al. Phys. Rev. D, 2004, **69**: 114021. hep-ph/0402204
- 4 Blaylock G, Seiden A, Nir Y. Phys. Lett. B, 1995, **355**: 555. hep-ph/9504306
- 5 Aubert B et al (BABAR). Phys. Rev. Lett., 2007, **98**: 211802. hep-ex/0703020
- 6 Staric M et al (Belle). Phys. Rev. Lett., 2007, **98**: 211803. hep-ex/0703036
- 7 Petrov A A. Int. J. Mod. Phys. A, 2006, **21**: 5686
- 8 YAO W M et al (Particle Data Group). J. Phys. G, 2006, **33**: 1
- 9 LIU T H. In Batavia 1994, The future of high-sensitivity charm experiments (Charm 2000), edited by Kaplan D, Kwan S. 1994. hep-ph/9408330
- 10 Bergmann S et al. Phys. Lett. B, 2000, **486**: 418. hep-ph/0005181
- 11 Aubert B et al (BABAR Collaboration). arXiv:0712.2249
- 12 Aubert B et al (BABAR). Phys. Rev. Lett., 2003, **91**: 121801. hep-ex/0306003
- 13 Kopp S et al (CLEO). Phys. Rev. D, 2001, **63**: 092001. hep-ex/0011065
- 14 Buccella F et al. Phys. Rev. D, 1995, **51**: 3478. hep-ph/9411286
- 15 Acosta D et al (CDF Collaboration). Phys. Rev. Lett., 2005, **94**: 122001; Aubert B et al (BABAR Collaboration). Phys. Rev. D, 2005, **71**: 091101
- 16 Grossman Y, Kagan A L, Nir Y. Phys. Rev. D, 2007, **75**: 036008
- 17 Aubert B et al (BaBar Collaboration). arXiv:0709.2715